An emulator for static and dynamic performance evaluation of small wind turbines

Adrien Prévost, Vincent Léchappé, Xavier Brun, Romain Delpoux

An emulator for static and dynamic performance evaluation of small wind turbines

Adrien Prévost
Univ Lyon, INSA Lyon
Universite Claude Bernard Lyon 1,
Ecole Centrale de Lyon,
Laboratoire Ampere CNRS UMR 5005
Villeurbanne, France
adrien.prevost@insa-lyon.fr

Vincent Léchappé
Univ Lyon, INSA Lyon
Universite Claude Bernard Lyon 1,
Ecole Centrale de Lyon,
Laboratoire Ampere CNRS UMR 5005
Villeurbanne, France
vincent.lechappe@insa-lyon.fr

Romain Delpoux
Univ Lyon, INSA Lyon
Universite Claude Bernard Lyon 1,
Ecole Centrale de Lyon,
Laboratoire Ampere CNRS UMR 5005
Villeurbanne, France
romain.delpoux@insa-lyon.fr

Xavier Brun
Univ Lyon, INSA Lyon
Universite Claude Bernard Lyon 1,
Ecole Centrale de Lyon,
Laboratoire Ampere CNRS UMR 5005
Villeurbanne, France
xavier.brun@insa-lyon.fr

***Abstract*—In this article, the modelling and control of a full scale Wind Turbine Emulator (WTE) was described for a 700 W rated power residential scale Wind Energy Conversion System (WECS). The WTE is made of a Permanent Magnets Synchronous Motor (PMSM) controlled by a Variable Frequency Drive (VFD). The PMSM is controlled in order to apply the torque of the blades directly on the generator. The differences between the test bench and the physical wind turbine in terms of mechanical parameters are taken into account. This is done by compensating the motor inertia and frictions with blades inertia through a reference speed trajectory tracking method. Experimental results with a Torque Meter (TM) confirmed that the aerodynamic torque is adequately applied on the generator by the WTE. The dynamic response was validated with torque steps and tested with turbulent wind. This emulator will help the development of advanced wind turbine control strategies and the comparison of different power conversion strategies for residential scale WECSs.**

***Index Terms*—wind turbine emulator, small scale wind turbine, mechanical dynamics emulation**

I. Introduction

Small scale WECS are used to power standalone off-grid systems or to feed power to the grid. In both cases, residential scale wind turbines (<20kW) are less competitive than their large scale counterparts because of a higher capital cost per power installed and a lower capacity factor [1]. Hence, a significant effort is made in the litterature to optimize small scale WECSs performance using various power conversion strategies [2]–[5]. The comparison of these strategies is difficult to undertake from the litterature data since different systems are studied. Moreover, various performance evaluation methods are used: simulation, laboratory bench testing, field-testing. The latter allows assessing a WECS real performance. However, it can require up to several months to meet the necessary experimental conditions to validate the performance of a power conversion strategy.

A real-time WECS emulator is a test setup that enables the replication of a real physical WECS by replacing some of its elements by controlled actuators or power electronics. Generally, the blades are replaced by a WTE which is an electrical machine whose torque is controlled to reproduce the aerodynamic torque. In some cases, the wind turbine generator is even replaced by a power electronics converter [6]. The use of a real-time WECS emulator can save a considerable amount of time in the development and comparison of power conversion strategies for wind turbines [7], [8], in particular because it enables to master the experimental conditions such as the weather conditions. Additionaly, some phenomena inherent to experimentation can be evidenced without risking damaging the real system [9].

However, the accurate replication of the physical WECS behavior with a WECS emulator is not straightforward. A particular attention should be taken to emulate the mechanical dynamics of the physical WECS. Indeed, it is known that generator and blades inertia have a significant influence on the performance of wind turbines [10], [11]. Moreover, the efficiency of the Electrical Generation System (EGS) (i.e. generator, lines and converter) also significantly affects the behavior of the WECS. Hence, to reflect the physical WECS performance with accuracy, the WECS emulator test bench should reproduce the real mechanical dynamics and have the same EGS as the physical WECS under study.

The work presented in this article is focused on the modelling and control of an experimental test bench to enable the comparison of several power conversion strategies for residential scale WECSs. For this purpose, a full scale generator-

in-the-loop WECS emulator test bed has been constructed. It consists of a PMSM driving a 700W rated power Locally Manufactured Small Wind Turbine (LMSWT) Permanent Magnets Synchronous Generator (PMSG) [12] which is connected to an active load through a rectifier. The PMSM is controlled to emulate the aerodynamic torque of the blades together with the dynamics caused by the inertia and frictions of the real physical WECS rotating system.

Using Bond Graph formalism, a particular attention is made to the mechanical modelling of the WECS and the test bed rotating systems, which are analyzed in Sections II and III. This analysis is then used in Section IV for the synthesis of the WTE control algorithm. Simulation and experimental results are compared in Section V to validate both static and dynamic mechanical behaviors of the WTE under steady and turbulent wind conditions.

II. The wind energy conversion system

A. System architecture

The architecture of the WECS under study is depicted in Fig. 1, it consists of a horizontal axis rotor with wind turbine blades directly mounted on an axial flux PMSG. The generator is connected to a battery bank through a rectifier. The rectifier could be either passive (diode bridge) or active (three legs voltage source converter). For the case of this article, a passive rectifier will be considered.

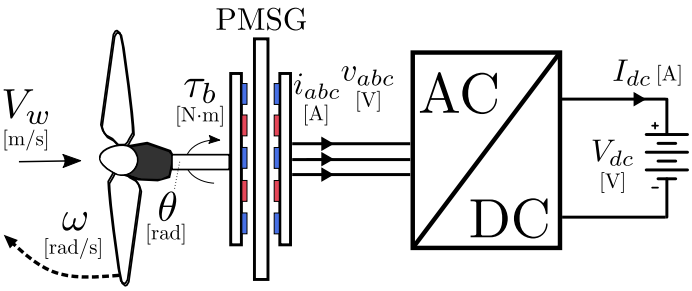

Fig. 1. WECS architecture.

B. Modelling of the WECS

1) The rotating system: Here, the modelling employs bond graph formalism which allows a fine visual understanding of the system causalities. This will be used to highlight the differences between the physical wind turbine and the WTE. The WECS rotating system is modelled with the bond graph represented in Fig. 2. On the left, a common flow (i.e. the blades angular velocity ω) 1-junction stands for the blades together with their inertia (J_b) represented by an I-element. The torque applied by the blades on the 1-junction is governed by aerodynamics and can be modelled by a modulated source of effort (MS_e) [13]. On the right, a common flow (i.e. generator angular velocity ω_g) 1-junction stands for the PMSG together with its inertia and damping coefficient represented by the I-element J_g and R-element b respectively. The PMSG electromagnetic torque τ_g applied on its 1-junction is modelled by a modulated source of effort. The mechanical connection between the blades and the PMSG is modelled by a common effort 0-junction with a stiffness k_s represented as a C-element. The resulting torque exchanged by the two common flow junctions is written as the shaft torque τ_s. The modelling of both sources of efforts will be addressed in the next two Sections.

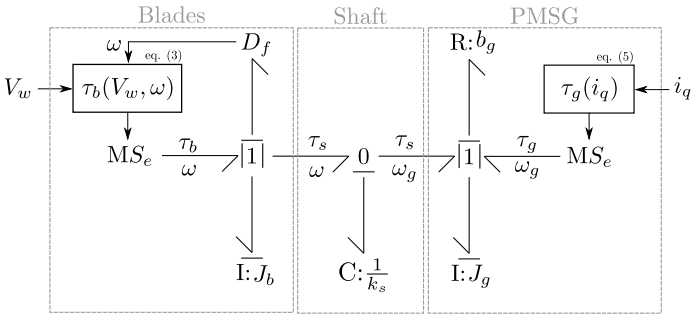

Fig. 2. Bond graph representation of the WECS blades and generator.

2) Rotor aerodynamics: Here, the modelling of the rotor aerodynamics focuses on the zone 2 WECS operation (i.e. between cut-in and rated wind speeds).

The aerodynamic efficiency of the wind turbine rotor is commonly modelled with the aerodynamic coefficient C_p which enables to write a static expression of the aerodynamic power extracted from the wind by the blades

$$P_{aero} = \frac{1}{2}\rho_{air} A V_w^3 C_p(\lambda), \tag{1}$$

with A the rotor swept area, ρ_{air} the air density, V_w the wind velocity and λ Tip Speed Ratio (TSR) given by

$$\lambda = \frac{\omega \cdot R}{V_w} \tag{2}$$

where ω is the rotor angular velocity and R the rotor radius.

The wind turbine blades under study have a fixed pitch, thus C_p varies in one dimension according to the TSR. The corresponding $C_p(\lambda)$ curve used in this paper was measured in situ on a LMSWT at the National Technical University of Athens, [14] and is given in Fig. 3.

By conservation of power, the aerodynamic torque from the blades can be written as

$$\tau_b = \frac{P_{aero}}{\omega}. \tag{3}$$

Assuming the shaft stiffness k_s is very important, it is possible to simplify the bond graph of Figure 2 by considering a single common flow junction with both PMSG (J_g) and blades (J_b) inertia as a single I-element ($J = J_b + J_g$). Hence, one can write the rotor dynamics as

$$J\frac{d\omega}{dt} = \tau_b + \tau_g - b_g\omega \tag{4}$$

with τ_g the electromagnetic torque applied by the PMSG and b_g the generator damping coefficient.

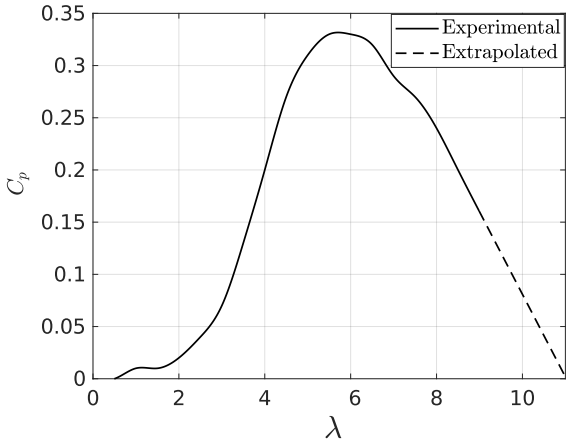

Fig. 3. LMSWT aerodynamic coefficient C_p in function of TSR λ.

3) Generator torque: The generator topology used in the LMSWT is an axial flux surface mounted PMSG with air-cored non-overlapping concentrated windings. The electromagnetic torque is given by

$$\tau_g = K_\tau i_q \tag{5}$$

with K_τ the torque coefficient (N·m/A) and i_q the quadrature axis current obtained through the Clarke and Park transformations [15] of the three-phase currents. The torque coefficient is given by

$$K_\tau = \frac{3}{2} p \phi_f \tag{6}$$

with ϕ_f the peak magnetic flux of the permanent magnets seen by a stator phase winding and p the pole pair number.

III. The WECS emulator

A. Emulator architecture

To reproduce the behavior of the WECS described above, the emulator represented in Fig. 4 was designed and constructed as a test bed. It consists of three elements: a Wind Turbine Emulator (WTE), a real scale Electrical Generation System (EGS) and a Load Emulator (LE). Each element is made of a hardware together with its control software layer. The WTE is composed of a PMSM which is controlled by a commercial VFD to emulate the dynamic torque applied by the blades on the generator. The EGS is made of a PMSG and a rectifier. The PMSG is real scale, meaning that it is made with the same design used for a 2.4 m rotor diameter LMSWT. The PMSM is mechanically connected to the PMSG through a TM which measures the shaft torque, angular velocity and position. The generator phase currents as well as DC-link voltage and rectifier output DC current are measured. Two rectifier options are available: passive or active, which enables the comparison of several conversion strategies. In this work, only the passive diode bridge rectifier is used. The load emulator consists of an active DC load which can be controlled to regulate the DC-link voltage, current or power. The rectifier is directly connected to the active DC load. The software layers are embedded in a dSPACE MicroLabBox which ensures the measurements acquisition and synthesis of control signals. Photos of the test bed are presented in Fig. 5 and Fig. 6.

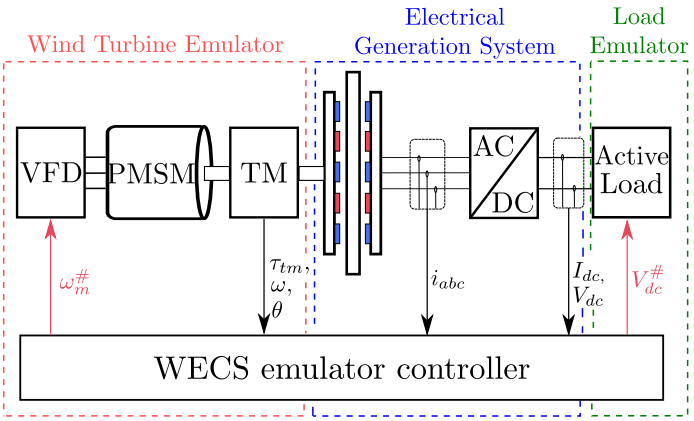

Fig. 4. Architecture of the WECS emulator with control signals (red) and measurements (black).

B. Modelling of the test bed

The bond graph in Fig. 7 represents the modelling of the test bed rotating system. Since a PMSM stands for the blades, the mechanical modelling of the emulator differs from the real WECS. Indeed, the motor inertia J_m differs from the blades' inertia J_b, and there is an additional damping coefficient b_m due to the motor bearings. The PMSM torque τ_m is modelled with a modulated source of effort controlled by the VFD. As for the PMSG, its modelling remains identical to the WECS bond graph since the generator is full scale. The TM stiffness k_{tm} allows the measurement of the common torque τ_{tm} which reflects the mechanical energy transfer between the two machines.

Assuming the TM and couplings rigidity is high enough to consider identical velocities on both machines, one can write $\omega_m = \omega_g = \omega$. Under this assumption, a single common flow

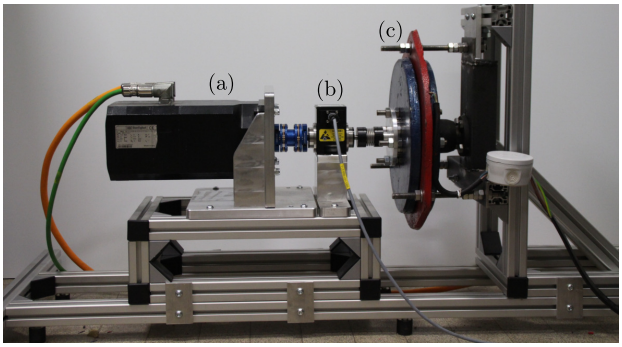

Fig. 5. The WECS emulator test bed : (a) PMSM, (b) TM, (c) PMSG.

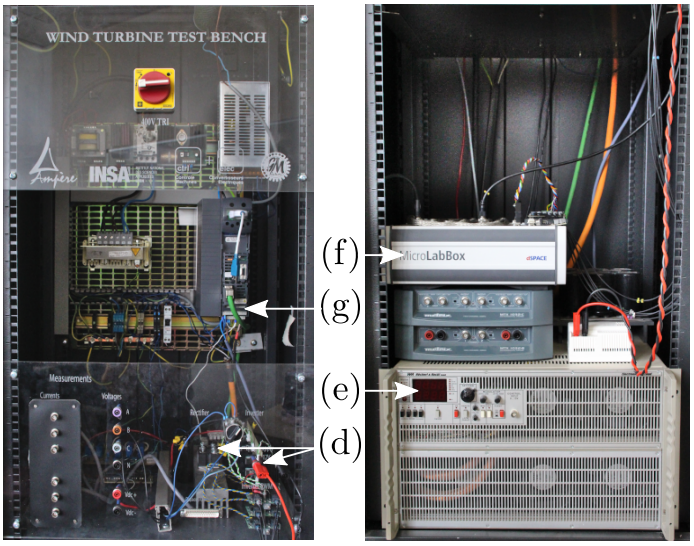

Fig. 6. The WECS emulator test bed : (d) rectifiers (passive and active), (e) active DC load, (f) MicroLabBox, (g) VFD.

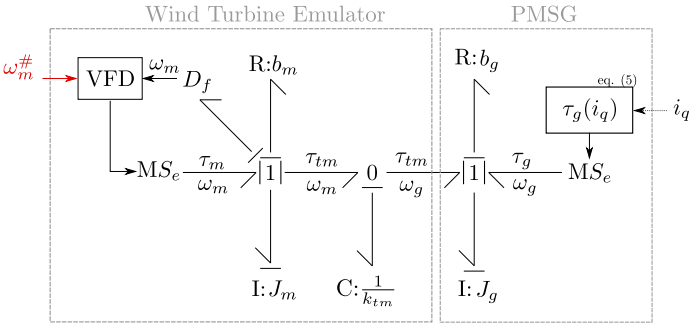

Fig. 7. Bond graph representation of the emulator mechanical subsystem.

junction on the PMSG side is considered, leading again to a one-mass equivalent system dynamics equation given by

$$(J_g + J_m)\frac{d}{dt}\omega = \tau_m + \tau_g - (b_g + b_m)\omega. \tag{7}$$

It can be seen that eq. (7) differs from eq. (4), hence the motor torque τ_m should be controlled to compensate for this difference.

IV. Wind Turbine Emulator Control

As mentioned previously, the emulator should reproduce both static and dynamic mechanical behaviors of the real wind turbine. The static behavior should be reproduced by emulating the blades aerodynamics while the dynamic behavior is achieved by emulating the mechanical parameters (J, b_g) of the real wind turbine. This implies the need of a specific wind turbine emulator control scheme which will be addressed here.

A. Aerodynamics emulation

The emulation of the blades aerodynamics is achieved using eqs. (1), (2) and (3) according to the simulator scheme in Fig. 8. The torque generated by the blades is computed in real-time according to the measured shaft angular velocity and the virtual wind velocity. In this work, the air density was chosen constant, however, it could be added as an input meteorological data varying in function of the time.

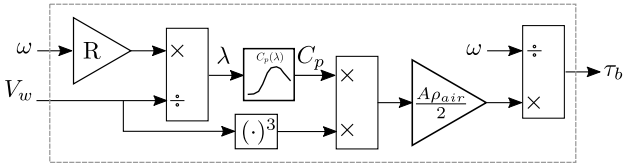

Fig. 8. Aerodynamics simulator scheme.

B. Mechanical dynamics emulation

As highlighted previously, the real WECS and the test bed are similar physical systems with different mechanical parameters. Thus, the test bed response to a fictive wind gust or to a generator dynamic torque variation will be different from the real WECS response if no compensation control law is employed. Typically, the real WECS velocity response will be slower than the test bed due to the blades additional inertia. A first way to emulate the dynamic torque of the wind turbine is to control the motor torque to compensate for the motor friction and inertia and add the extra inertia of the blades. This could be done by following the torque reference

$$\tau_m^{\#}(\omega) = (J_m - J_b)\frac{d\omega}{dt} + b_m\omega + \tau_b(\omega). \tag{8}$$

However, this requires a differentiator which is highly sensitive to noise and can bring instabilities issues [16]. Moreover, it requires a perfect knowledge of J_m and b_m. In [17], a similar dynamic load torque compensation strategy is used to simulate the blades' inertia without the need of a differentiator. This method requires a very good knowledge of the PMSM and PMSG parameters and does not allow considering a damping coefficient different from the generator coefficient. For these reasons, another type of method was chosen : controlling directly the angular velocity of the PMSM, following the "model speed tracking" principle [9]. By integration of eq. (4), it is possible to generate an angular velocity reference trajectory corresponding to the response of the one-mass equivalent rotating system with the desired set of parameters to emulate (J_e, b_e). The motor velocity reference trajectory is given by

$$\omega_m^{\#} = \frac{1}{J_e}\int(\tau_b + K_\tau i_q - b_e\omega)dt. \tag{9}$$

which is implemented on the test bed controller according to the scheme in Fig. 9 and sent to the VFD. The speed controller will not be detailed here since it is embedded in the commercial VFD. In order to get the aerodynamic torque being directly applied on the generator, one should set $b_e = b_g$ which leads the controller to compensate the frictions of the PMSM. A significant advantage of this speed tracking method is the exact knowledge of the emulated mechanical parameters,

which enables to compare simulation and experimentation easily as it will be done in the next Section.

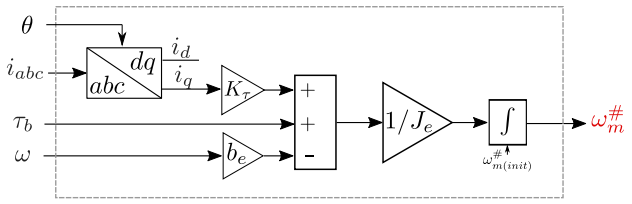

Fig. 9. Mechanical dynamics emulation control scheme.

V. Experimental Results and Discussions

A. Static behavior

The aerodynamic torque in function of the rotational speed has been computed analytically with equations (1), (2), (3) and plotted on Fig. 10 (solid lines). To validate that the emulator is adequately reproducing the aerodynamic torque, the torque at the TM shaft was measured for different DC voltages at the diode rectifier for a same wind speed. The experiment was conducted for low, medium and high wind speeds. This resulted in different torque and speed measured operating points which are plotted in orange on the same figure. One can see that the emulator operating points adequately fit the calculated aerodynamic torque.

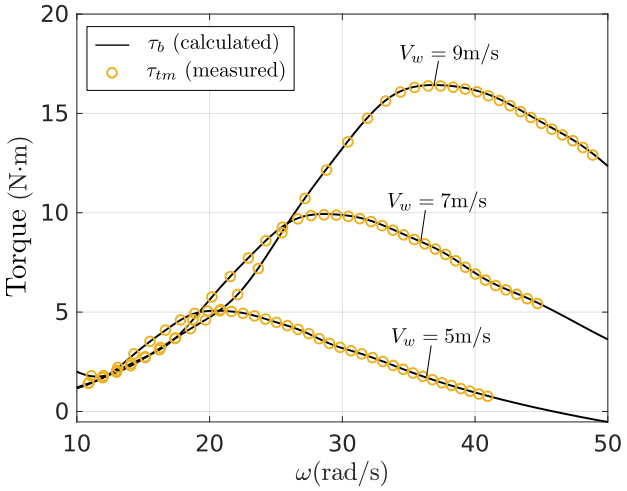

Fig. 10. Comparison between the calculated aerodynamic torque and the torque measured on test bench under static wind conditions.

B. Dynamic behavior

The WECS emulator rotational velocity response to a wind gust (red curve in Fig. 11-Bottom) and then to a generator torque step (blue curve in Fig. 11-Bottom) was tested experimentally for two different emulated inertia (without and with blades inertia). Here the generator torque is deduced from the stator currents. The resulting velocity responses are represented in Fig. 11-Top and compared to simulation. The WECS emulator responses fit adequately the simulated desired behaviors (in dashed lines).

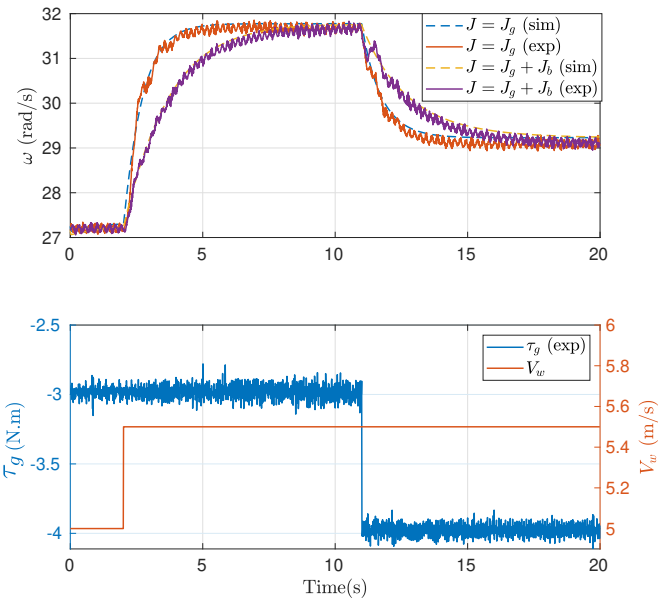

Fig. 11. Response of the emulator to a wind gust and a generator torque step for two different inertia values.

To test the emulator under realistic wind conditions, a turbulent wind was generated with the TurbSim software and injected in the emulator. A Kaimal turbulence model with a mean wind speed of 6 m/s, a surface roughness length of 0.25 and a hub height of 15 m were used, which are realistic parameters for residential scale WECSs. The wind speed in function of the time is plotted at the top of the graph in Fig. 12. The corresponding torque and rotational velocity of the emulator under passive rectification with a fixed DC voltage are plotted for two scenarios of system inertia. The response of the emulator without blades inertia emulation shows that the torque follows the transient dynamics of the wind. As expected, when the blades' inertia is emulated, the aerodynamic torque is filtered by the inertia resulting in a smoother torque transmitted to the generator. As a result, a significant influence on the rotational velocity can be observed, which shows smoother transients in comparison to the experiment without blades inertia emulation. Since the TSR is directly linked to the rotational velocity, this phenomenon has a direct influence on the aerodynamic coefficient of the wind turbine which impacts the whole power conversion chain. This highlights the importance to take into account this phenomenon when assessing power performance with a WECS emulator.

VI. Conclusion

The use of a real-time WECS emulator can fasten the development and testing of WECSs power conversion strategies. In this work, a full scale WECS emulator (i.e. a WTE, a real

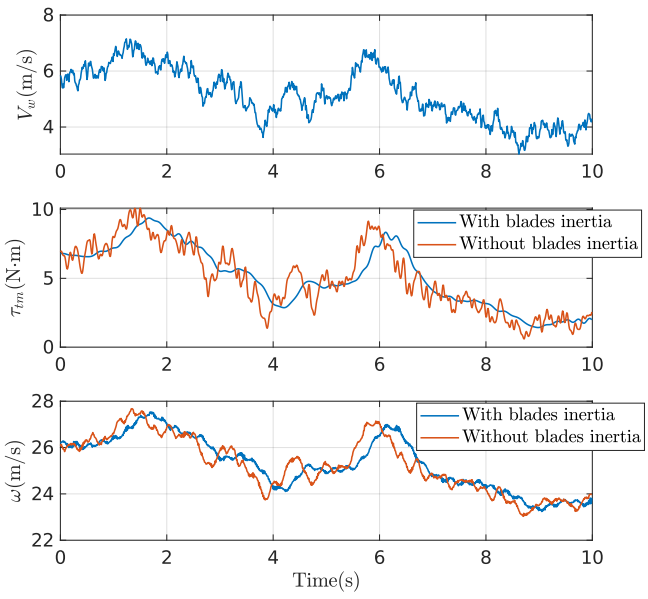

Fig. 12. WECS emulator mechanical behavior under turbulent wind conditions, with and witout blades inertia.

Parameter	Name	Value	Unit
J_m	PMSM inertia	$1.28 \cdot 10^{-3}$	kg.m^2
J_b	Blades inertia	0.378	kg·m^2
J_g	PMSG inertia	0.28	kg·m^2
b_g	PMSG damping coefficient	0.01	N·m·s/rad
R	Blades length	1.2	m

TABLE I
WECS AND EMULATOR PHYSICAL PARAMETERS.

scale wind turbine generator, its converter and a load) was implemented for a 700 W rated power residential scale WECS. The modelling and control of the WTE was described. The control of the WTE was designed to apply the torque of the blades directly on the generator by simulating in real-time the aerodynamic torque and controlling a motor to mimic it. The differences between the test bench and the physical WECS in terms of mechanical dynamics were taken into account. This was done by compensating the motor inertia and frictions with blades inertia through a reference speed trajectory tracking method. Experimental results confirmed that the aerodynamic torque is adequately applied on the generator by the WTE. Additionally, the dynamic response was validated with torque steps and tested under turbulent wind. This WECS emulator will help the development of advanced wind turbine control strategies with maximum power point tracking and the comparison of different power conversion strategies including active synchronous rectification. Future works will involve field-testing to compare the behavior of the emulator and the physical WECS. This will help to determine to which extent the emulator is accurate and if further phenomena should be included in the emulation of torque, like the tower shadow and wind shear effects.

ACKNOWLEDGMENT

The authors would like to thank Jay Hudnall for providing the LMSWT generator and Bertrand Richert for his kind advice with TurbSim.

REFERENCES

[1] E. Lantz, B. Sigrin, M. Gleason, R. Preus, and I. Baring-Gould, "Assessing the Future of Distributed Wind: Opportunities for Behind-the-Meter Projects," Tech. Rep. NREL/TP–6A20-67337, 1333625, Nov. 2016.

[2] B. Sareni, A. Abdelli, X. Roboam, and D. Tran, "Model simplification and optimization of a passive wind turbine generator," *Renewable Energy*, vol. 34, no. 12, pp. 2640–2650, Dec. 2009.

[3] R. Aubrée, F. Auger, M. Macé, and L. Loron, "Design of an efficient small wind-energy conversion system with an adaptive sensorless MPPT strategy," *Renewable Energy*, vol. 86, pp. 280–291, Feb. 2016.

[4] K. Latoufis, G. Serafeim, K. Chira, V. Riziotis, S. Voutsinas, and N. Hatziargyriou, "Holistic Design of Small-scale Stand-alone Wind Energy Conversion Systems Using Locally Manufactured Small Wind Turbines," *Journal of Physics: Conference Series*, vol. 1618, p. 042012, Sep. 2020.

[5] C. J. J. Labuschagne and M. J. Kamper, "Wind Generator Impedance Matching in Small-Scale Passive Wind Energy Systems," *IEEE Access*, vol. 9, pp. 22 558–22 568, 2021.

[6] D. H. Wollz, S. A. O. da Silva, and L. P. Sampaio, "Real-time monitoring of an electronic wind turbine emulator based on the dynamic PMSG model using a graphical interface," *Renewable Energy*, vol. 155, pp. 296–308, Aug. 2020.

[7] P. E. Battaiotto, R. J. Mantz, and P. F. Puleston, "A wind turbine emulator based on a dual dsp processor system," p. 6, 1996.

[8] N. R. Averous, M. Stieneker, S. Kock, C. Andrei, A. Helmedag, R. W. De Doncker, K. Hameyer, G. Jacobs, and A. Monti, "Development of a 4 MW Full-Size Wind-Turbine Test Bench," *IEEE Journal of Emerging and Selected Topics in Power Electronics*, vol. 5, no. 2, pp. 600–609, Jun. 2017.

[9] H. Camblong, I. M. de Alegria, M. Rodriguez, and G. Abad, "Experimental evaluation of wind turbines maximum power point tracking controllers," *Energy Conversion and Management*, vol. 47, no. 18-19, pp. 2846–2858, Nov. 2006.

[10] C. Tang, M. Pathmanathan, W. L. Soong, and N. Ertugrul, "Effects of Inertia on Dynamic Performance of Wind Turbines," *Australasian Universities Power Engineering Conference*, p. 7, 2008.

[11] M. Nasiri, J. Milimonfared, and S. Fathi, "Modeling, analysis and comparison of TSR and OTC methods for MPPT and power smoothing in permanent magnet synchronous generator-based wind turbines," *Energy Conversion and Management*, vol. 86, pp. 892–900, Oct. 2014.

[12] H. Piggott, *A Wind Turbine Recipe Book*, 2009.

[13] T. Bakka and H. R. Karimi, "Wind turbine modeling using the bond graph," in *2011 IEEE International Symposium on Computer-Aided Control System Design (CACSD)*. Denver, CO, USA: IEEE, Sep. 2011, pp. 1208–1213.

[14] National and Technical University of Athens, "Aerodynamic Coefficient | OpenWindLab," 2023. [Online]. Available: https://openwindlab.net/#/graphs/aerodynamic-coefficient/2

[15] R.-H. Park, "Two-reaction theory of synchronous machines generalized method of analysis-part I," *Transactions of the American Institute of Electrical Engineers*, vol. 48, no. 3, pp. 716–727, 1929.

[16] L. Weijie, Y. Minghui, Z. Rui, J. Minghe, and Z. Yun, "Investigating instability of the wind turbine simulator with the conventional inertia emulation scheme," in *2015 IEEE Energy Conversion Congress and Exposition (ECCE)*. Montreal, QC, Canada: IEEE, Sep. 2015, pp. 983–989.

[17] J. Yan, Y. Feng, and J. Dong, "Study on dynamic characteristic of wind turbine emulator based on PMSM," *Renewable Energy*, vol. 97, pp. 731–736, Nov. 2016.